Int J Adv Manuf Technol (2008) 37:471–485
DOI 10.1007/s00170-007-0986-z

ORIGINAL ARTICLE

Development of a cutting tool condition monitoring system for high speed turning operation by vibration and strain analysis

H. Chelladurai · V. K. Jain · N. S. Vyas

Received: 13 December 2006 / Accepted: 19 February 2007 / Published online: 23 March 2007

Abstract Cutting tool wear is a critical phenomenon which influences the quality of the machined part. In this paper, an attempt has been made to create artificial flank wear using the electrical discharge machining (EDM) process to emulate the actual or real flank wear. The tests were conducted using coated carbide inserts, with and without wear on EN-8 steel, and the acquired data were used to develop artificial neural networks model. Empirical models have been developed using analysis of variance (ANOVA). In order to analyze the response of the system, experiments were carried out for various cutting speeds, depths of cut and feed rates. To increase the confidence limit and reliability of the experimental data, full factorial experimental design (135 experiments) has been carried out. Vibration and strain data during the cutting process are recorded using two accelerometers and one strain gauge bridge. Power spectral analysis was carried out to test the level of significance through regression analysis. Experimental results were analyzed with respect to various depths of cut, feed rates and cutting speeds.

Keywords Artificial flank wear · Strain · Vibration · Empirical model · EDM · Metal cutting · Cutting tool condition monitoring

1 Introduction

In the last three decades or so, there have been tremendous improvements and technical revolutions in manufacturing industries, namely computer integrated manufacturing process, robot controlled machining processes, and others. Today customer demands high quality products for lowest possible price. To meet customers' such demands and to face global competition, modern industries are facing various challenges towards achieving high dimensional accuracy with mirror surface finish on the products. To achieve such goals the manufacturers are focusing on the technical problems namely, how to achieve uninterrupted automated machining process for longer duration with least human supervision. Cutting tool wear condition monitoring is an important technique that can be useful especially in automated cutting processes and unmanned factories to prevent any damage to the machine tool and workpiece. In any metal cutting operation, one of the major hurdles in realizing its complete automation is that of the cutting tool-state prediction, where tool-wear is a critical factor in productivity. Cutting tool condition monitoring can help in on-line realization of the tool wear, tool breakage, and workpiece surface roughness.

Researchers and engineers have been trying to evolve a cutting tool condition monitoring system with high reliability [1]. There is a need for reliable, universal cutting tool condition monitoring (TCM) system, which is suitable for industrial applications. Various sensing techniques [2] have been reported in the literature by various investigators which deal with the issues of detecting edge chipping, fracture, tool wear and surface finish. Many sensors were adopted in the area of metal cutting tool condition monitoring system namely, touch sensors, power sensors, acoustic emission sensors [3–6], vibration sensors, torque sensors, force sensors, vision sensors and so on. In any automation process, sensors and their signal interpretation play an important role. The processing and analysis of signals is important because it will improve production

H. Chelladurai · V. K. Jain (✉) · N. S. Vyas
Department of Mechanical Engineering,
Indian Institute of Technology Kanpur,
Kanpur 208016, India
e-mail: vkjain@iitk.ac.in

capacity, reliability, reduced downtime and improved machining quality [7]. Sensors and their utilization were implemented in many areas like machine tool, automotive, and tool manufacturing. Byrne et al. [8] reported that 46 % of the sensors monitoring systems were fully functional, 16% had limited functionality, 25% of the systems were non-functional due to technical limitations and 13% were replaced by or switch over to alternate systems. It should be noted that, in sensors based systems the most critical decision is prediction of cutting tool condition using signal response. In many cases wrong interpretation of the sensor signals by an operator leads to the wrong decision to switch off the machine tool which affects the quality of the product as well as production rate. The training of the personnel also plays a vital role in successful implementation of tool condition monitoring systems.

Generally, machining processes are non-linear and stochastic in nature, and it is difficult to build a mathematical model, which requires suitable assumptions and may not be matching with real world metal cutting process. An intensive research has been carried out related to TCM system covering various metal cutting processes such as turning, milling, drilling and grinding, over the past two decades or so [9]. A good cutting tool condition monitoring system [10] should be characterized by (a) fast detection of impact or collisions, (i.e., unwanted movement between tool and workpiece, or tool and any other component of the machine tool), (b) tool chipping (cutting edge breakage), and (c) gradual tool wear (crater and flank) caused by abrasion due to friction between cutting tool and workpiece (flank wear) and cutting tool and chip (crater wear).

Tool wear sensing techniques are broadly classified into two categories: direct and indirect as shown in Table 1. The direct tool wear monitoring methods can be applied when cutting tools are not in contact with the work piece [11] like radioactive, microscope, camera vision and so on. However, direct methods of measuring tool wear have not been easily adaptable for shop floor application. They are not suitable for on-line condition monitoring system however they can be easily applied to off-line measurements and it consumes more time. Indirect tool sensing methods use relationship between cutting conditions and response of machining process which is a measurable quantity through sensor signals output (such as force, acoustic emission, vibration, or current) and may be used to predict the condition of the cutting tool. These indirect methods are used extensively by various researchers and the detailed analyses have been carried out in the past two decades. These indirect methods can be implemented to an industrial problem, but they have a lower sensitivity compared to direct methods. Nowadays, availability of computational power and reliability of electronics help in the development of a reliable condition monitoring system by using indirect methods. However, a problem in TCM system is selection of proper sensor and its location. The sensors have to be placed as close as possible to the target location (close to the tool tip) being monitored.

Table 1 Tool wear sensing methods

Direct methods	Indirect methods
-Electrical resistance	-Torque and power
-Optical measurements	-Temperature
-Radio active	-Vibration & acoustic emission
-Contact sensing	-Cutting forces & strain measurements

It is interesting to note that an indirect TCM system [12] consists of four steps: (i) collection of data in terms of signals from sensors such as cutting force, vibration, temperature, acoustic emission and/or motor current, (ii) extraction of features from the signals, (iii) classification or estimation of tool wear using pattern recognition, fuzzy logic, neural networks, or regression analysis, and (iv) development of an adaptive system to control the machining process based on information from the sensors.

There have been many investigations on tool wear based on periodic measurements of wear levels using optical microscope. In the present study, artificial wear has been created (externally) using electric discharge machining (EDM) process in a controlled manner. This is similar to a real flank wear experienced by the tool during machining process. Using this (artificially worn) cutting tool, cutting experiments are performed and signals are captured. This paper aims to develop a systematic feature extraction procedure from the output responses (accelerometers and strain gauges) of a machining process. These features are then fed as inputs to the back propagation feed forward neural networks, for classification or estimation of tool wear. Same experimental data were fed as inputs to the analysis of variance (ANOVA) to test the level of significance. The regression empirical models have been developed and validated with experimental results.

2 Creation of artificial wear

The cutting tool failure [8] can be classified into two categories: (a) gradual wear due to loss of material on an asperity or micro contact between cutting tool and workpiece which causes friction and leads to tool failure after a certain time interval, and (b) premature cutting edge failure due to chipping which occurs suddenly due to improper selection of machining parameters or tool material defect, or both. If a cutting tool approaches towards the end of its useful life, surface quality of the machined work piece is likely to deteriorate [1]. Characteristics of the surface

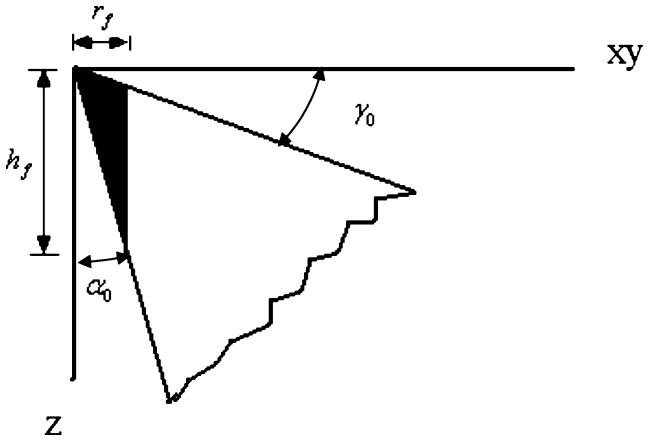

Fig. 1 Flank wear forms

topography of a machined work piece depend on the condition of the cutting tool including tool geometry, cutting tool material, work piece material, cutting conditions (with or without cooling) and machining parameters (cutting speed, feed rate and depth of cut). In general, the single point turning tool is subjected to different types of wear such as flank wear, crater wear, nose wear and chipping. Out of these wears, flank wear is considered in the present work although others are equally important under different machining conditions. While creating artificial flank wear, the following important cutting tool geometrical parameters are taken into consideration like rake angle, clearance angle, length of the flank wear and radial wear length [13].

The relation between flank wear and radial wear is given (Fig. 1) by

$$r_f = \frac{h_f \tan \alpha_0}{1 - \tan \gamma_0 \tan \alpha_0} \tag{1}$$

where, r_f is radial wear, h_f is flank wear, α_0 is clearance angle and γ_0 is rake angle.

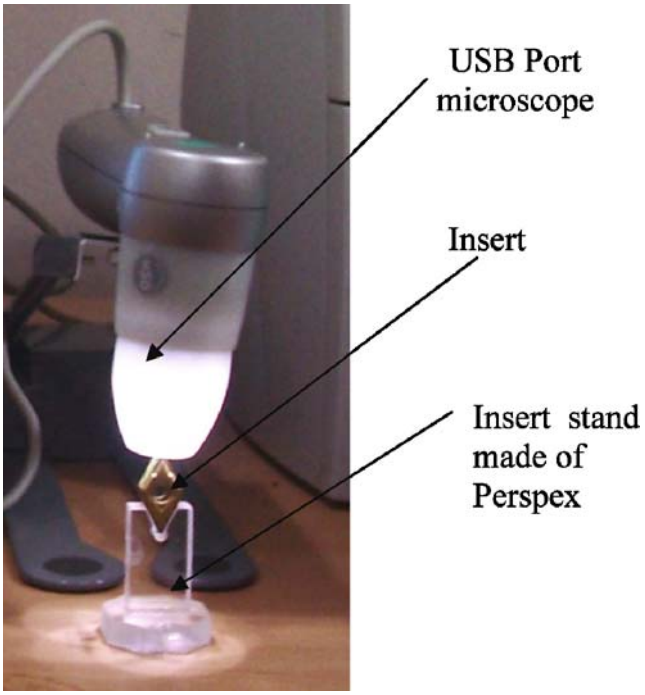

Fig. 3 Flank wear measurements

According to Eq. (1), the value of depth of cut (h_f) and radial distance (r_f) are calculated to create flank wear in the range of 0.2 mm to 0.5 mm. EDM experimental setup is used to create artificial flank wear. The replica of the flank wear is first produced in the copper rod by turning operation and then the copper rod is used in the EDM process as a tool (cathode) to replicate the flank wear on the cutting tool. During EDM, the tungsten carbide cutting tool (used as a work piece in EDM operation) is made as an anode. Machining parameters values are chosen in terms of feed rate as well as depth of cut to create exact shape of flank wear as shown in Fig. 2. The measurement of wear can be carried out using one of the three categories of

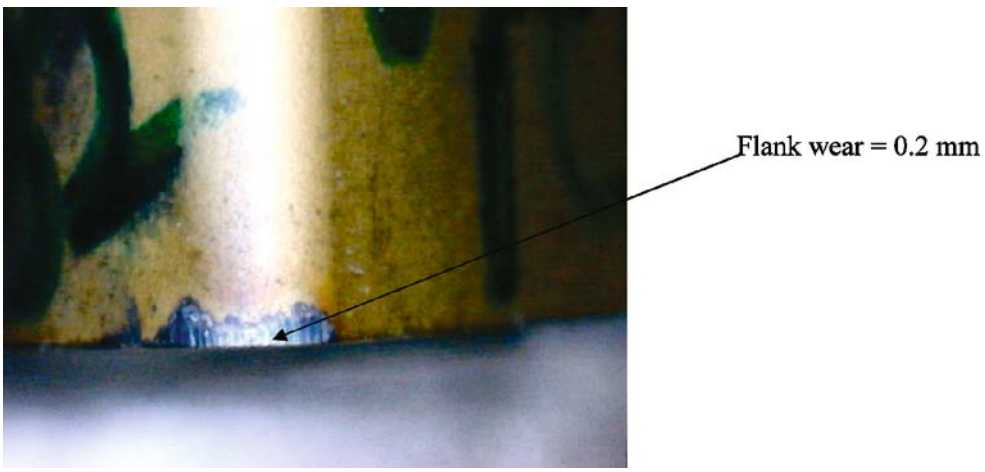

Fig. 2 Artificial flank wear created by EDM process

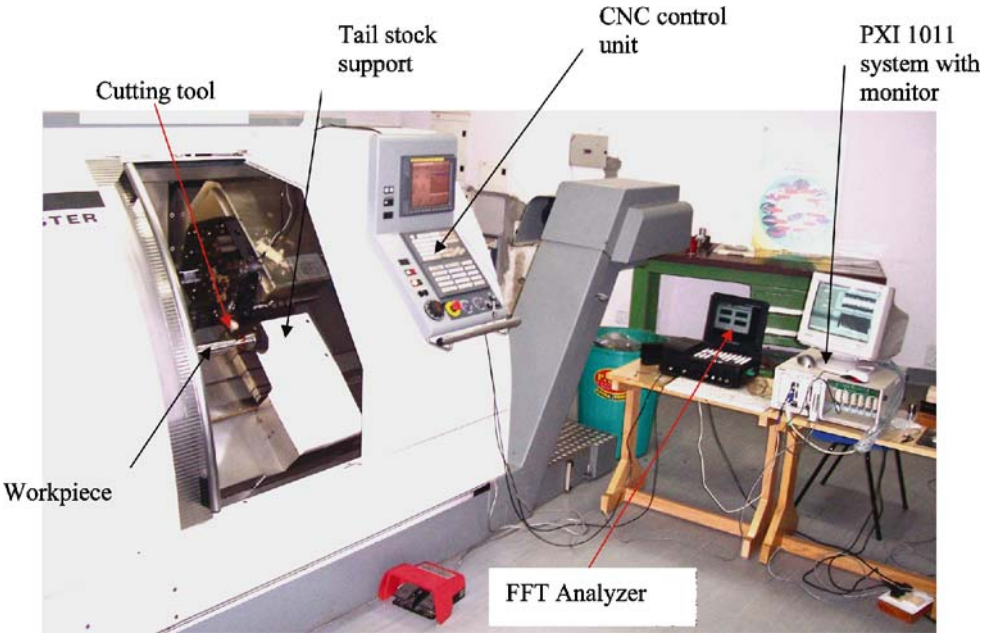

Fig. 4 Experimental setup

sensors, namely proximity sensors, radioactive sensors and vision sensors. Most of the researchers use an optical microscope to determine worn out areas, like flank wear length and crater wear length.

In this study, optical USB port microscope (Scalar) is used to capture the image of worn out area with magnification factor of 50x. Before measurements, insert is mounted on a stand, made of Perspex having included angle of 55° as shown in Fig. 3. It covers the entire portion of nose and flank face. Through out the measurements, position of the stand and focal distance are kept constant so that uniform measurements are achieved without any variation. In this microscope, built-in software (namely USB digital scale) is used to measure the flank wear.

3 Experimentation

Experiments were carried out on a CNC Gildemeister CTX 400 Serie 2 turning centre. The experimental setup is shown in Fig. 4. Experiments were conducted on EN-8 steel using DNMG 150608 insert with Seco tool holder PDJNR 2020 K15 without cutting fluid. The tool is instrumented with strain gauges (TML-120Ω) and two accelerometers (NP-3331-ONO-SOKKI). The strain gauge signals are taken to a PXI system and accelerometer signals are taken to an ONOSOKKI FFT analyzer. The PXI system is equipped with a Wheatstone bridge configuration and an amplifier. The magnitude of strain and amplitude of vibration depend upon various machining parameters and it is observed that they increase with depth of cut and feed rate, and decrease with cutting speed. While machining, the cutting tool is subjected to a state of stress. The resultant strain induces a voltage signal and it is measured with a half bridge configuration using LabVIEW.

Two accelerometers were placed in the turning centre. One was placed in the cutting direction on the tool holder, and the other one was placed in the feed direction on the

Table 2 Independent variables

Variables	Unit	Levels				
		1	2	3	4	5
Cutting speed	m/min	200	350	500		
Feed rate	mm/min	100	300	500		
Depth of cut	mm	3	4	5		
Flank wear	mm	0	0.2	0.3	0.4	0.5

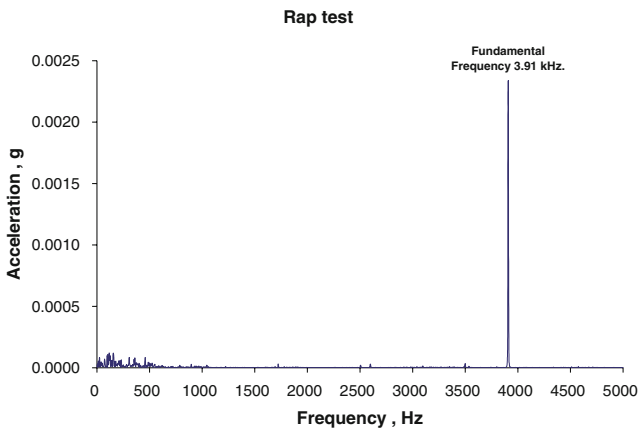

Fig. 5 Rap test for cutting tool

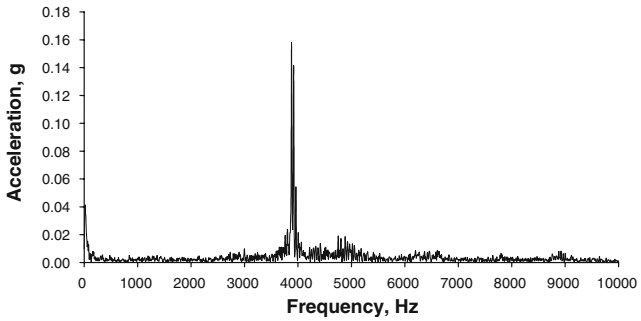

Fig. 6 Cutting speed=200 m/min, feed=500 mm/min and depth of cut=3 mm for flank wear 0.3 mm. Response of the accelerometer in cutting direction

backside of the turret for measuring vibration amplitude in terms of accelerations (g-levels).

3^k full factorial design [14] with three levels for each value of factors k is used. The three levels of factors are low (−1), intermediate (0), high (1). It forms 3^3 factorial designs and it contains 27 experiments with degrees of freedom equal to 26. A full factorial design was selected to allow all the three level interactions between the independent variables to be effectively investigated. The independent variables in this study are cutting speed, feed rate and depth of cut. The artificial flank wear is the fourth independent variable kept at five different levels ranging from 0 to 0.5 mm as shown in Table 2.

The three responses or dependent variables (strain due to bending action of a cutting tool, acceleration in cutting direction and acceleration in feed directions) are measured for various machining conditions. Tungsten carbide cutting tools equipped with throw-away inserts (DNMG 150608) were used in turning operation. Based on the previous study [15], flank wear level is minimum at the tool corner radius of 0.8 mm. So, in this study, the insert nose radius has been chosen as 0.8 mm with an angle of 55° diamond shape. The work piece material is EN8 steel and is supported by a tailstock to avoid excessive overhang. A total number of 135 experiments were performed to include all combinations of the four independent parameters.

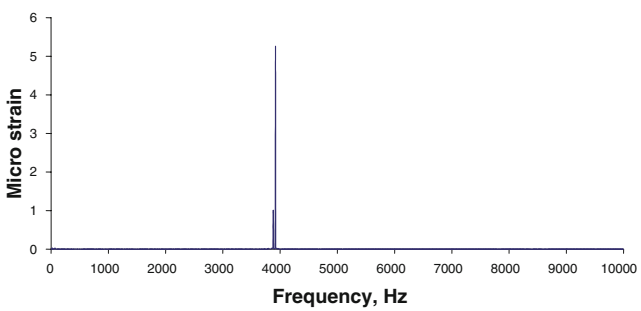

Fig. 7 Cutting speed=200 m/min, feed=500 mm/min and depth of cut=3 mm for flank wear 0.3 mm. Response of the strain gauge

Dynamometers can measure the static and dynamic forces accurately and they can be used [16] as a part of cutting tool condition monitoring systems. But, their frequency range is usually limited by the natural frequency f_0 of piezoelectric components of about 3 kHz. In order to avoid amplitude distortion, the usable frequency of a piezoelectric transducer is restricted to about 0.6 times of f_0. In view of this, an attempt has been made to measure

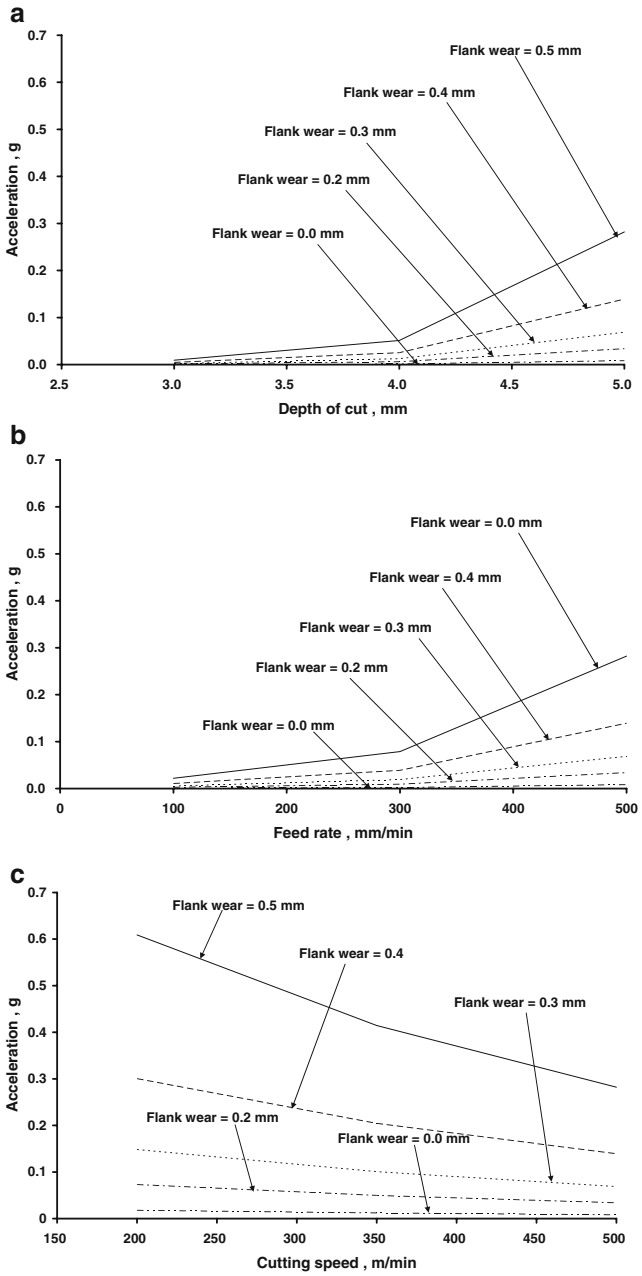

Fig. 8 **a** Regression model responses (channel 1) cutting speed=500 m/min and feed rate=500 mm/min. **b** Regression model responses (channel 1) cutting speed=500 m/min and depth of cut=5 mm. **c** Regression model responses (channel 1) feed rate=500 mm/min and depth of cut=5 mm

both static and dynamic components of cutting force using resistance type strain gauges (TML-120Ω -3 mm gauge length). Such gauges can follow the static and dynamic response of a system up to 350 kHz. These strain gauges are economical and get easily pasted on the surface of the tool. Also, they do not affect the stiffness of the tool holder.

Several references are available [17] on vibrations in the low frequency range, close to the natural frequency of vibration of spindle work piece (up to 300 Hz). Various authors have found that the frequencies relevant for TCM can be as high as 8 kHz, and usually above 1 kHz. This means that the signal essentially, consists of low frequency components that are indicators of static cutting forces. In the higher frequency range, natural frequencies of the tool holder are observed. The forces in this range (higher frequency) are called as dynamic cutting forces. In the present work, the fundamental natural frequency of the cutting tool was found to be 3.91 kHz, by conducting a rap test as shown in Fig. 5. Experiments have been carried out

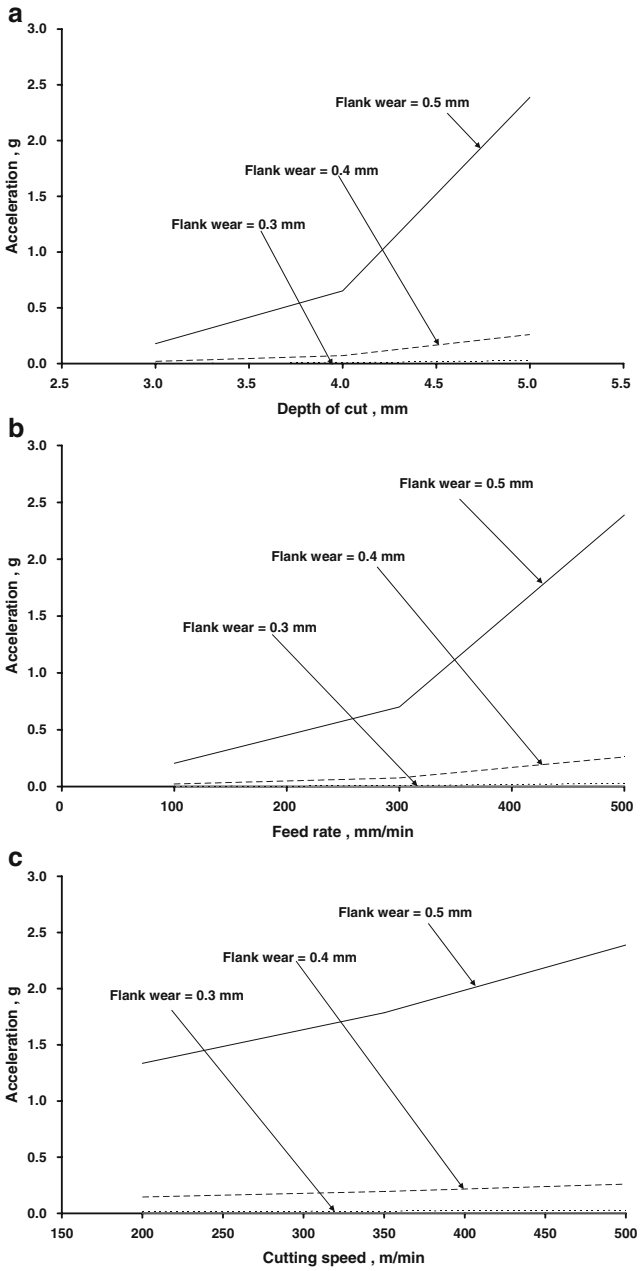

Fig. 9 **a** Regression model responses (channel 2) cutting speed=500 m/min and feed rate=500 mm/min. **b** Regression model responses (channel 2) cutting speed=500 m/min and depth of cut=5 mm. **c** Regression model responses (channel 2) feed rate=500 mm/min and depth of cut=5 mm

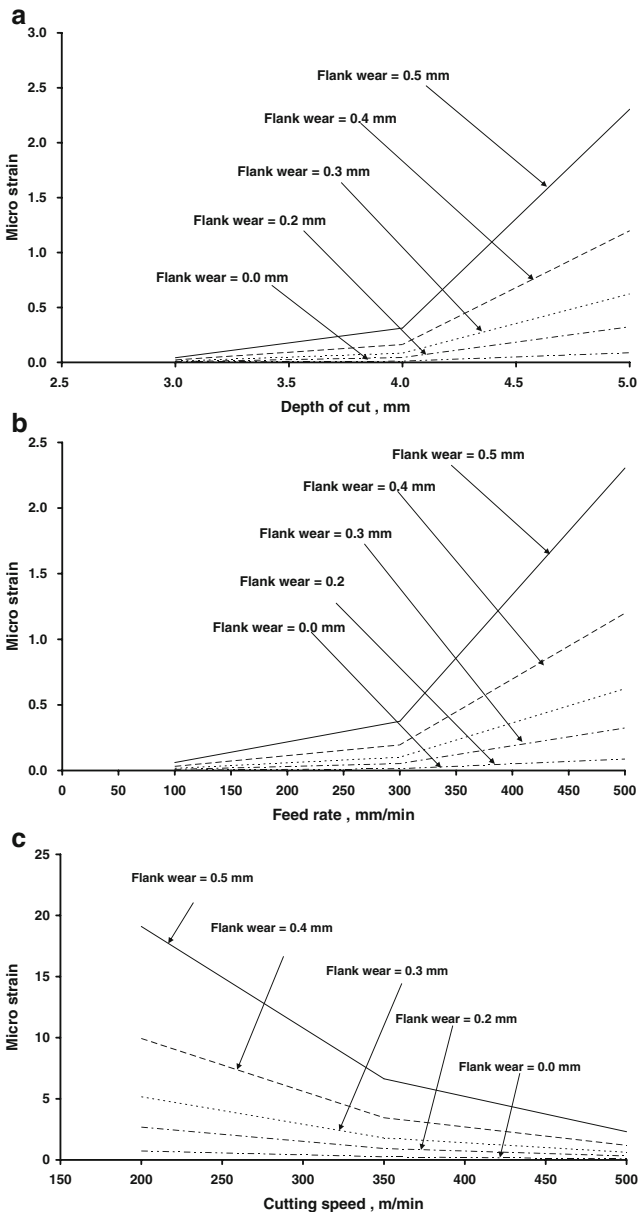

Fig. 10 **a** Regression model responses (channel 3) cutting speed=500 m/min and feed rate=500 mm/min m/min and depth of cut=5 mm. **b** Regression model responses (channel 3) cutting speed=500 m/min and depth of cut=5 mm. **c** Regression model responses (channel 3) feed rate=500 mm/min and depth of cut=5 mm

for various machining conditions. Strain gauge and vibration signals are measured from 0 to 10 kHz with a sampling rate of 25.6 kHz. Sample size is 4096 data points. Programming is done in LabVIEW to acquire the strain gauge signals and store them continuously frame by frame to monitor the condition of the cutting tool at every stage in on-line.

4 Results and discussions

The cutting phenomenon has been analyzed by using power spectrum of vibration and strain gauge signals. Typical power spectral plots are shown in Figs. 6 and 7. It is seen that 3.91 kHz is the predominant frequency in the response signals. Input parameters (amplitude of acceleration, *g* and strain) to the ANOVA are obtained from the three sensors output using MatLab code as shown in the Appendix 1 (Tables 6, 7 and 8) and the models are described in the later part of this section.

In order to develop an empirical model, statistical analysis is performed on the experimental data to determine the most significant input parameters (cutting speed, feed and depth of cut) with respect to the responses (output parameters). In this analysis, three empirical models have been proposed using three sensors responses: (I) accelerometer response in cutting direction (channel 1), (ii) accelerometer response in feed direction (channel 2) and (iii) strain gauge bridge response (channel 3). The criterion for the selection of a model had been the highest value of coefficient of correlation among the models that were fitted. It is observed that, vibration and strain gauge signals peaks exhibit response in a particular dynamic frequency range (3.8 kHz to 4.1 kHz) with respect to various machining conditions. The damping characteristics of the turning tool have been studied under dynamic conditions in the above said frequency range. The effects of three cutting parameters on the three response parameters are discussed below.

4.1 Effect of depth of cut on acceleration, *g* and strain

The relation between acceleration, *g* and depth of cut for various flank wear levels are as shown in Figs. 8a and 9a. The tool vibration increases with increase in depth of cut as well as increase in flank wear. This is due to an increase in cutting force which reduces stiffness of the cutting tool. It is observed that, in all cases the amplitude of vibration in

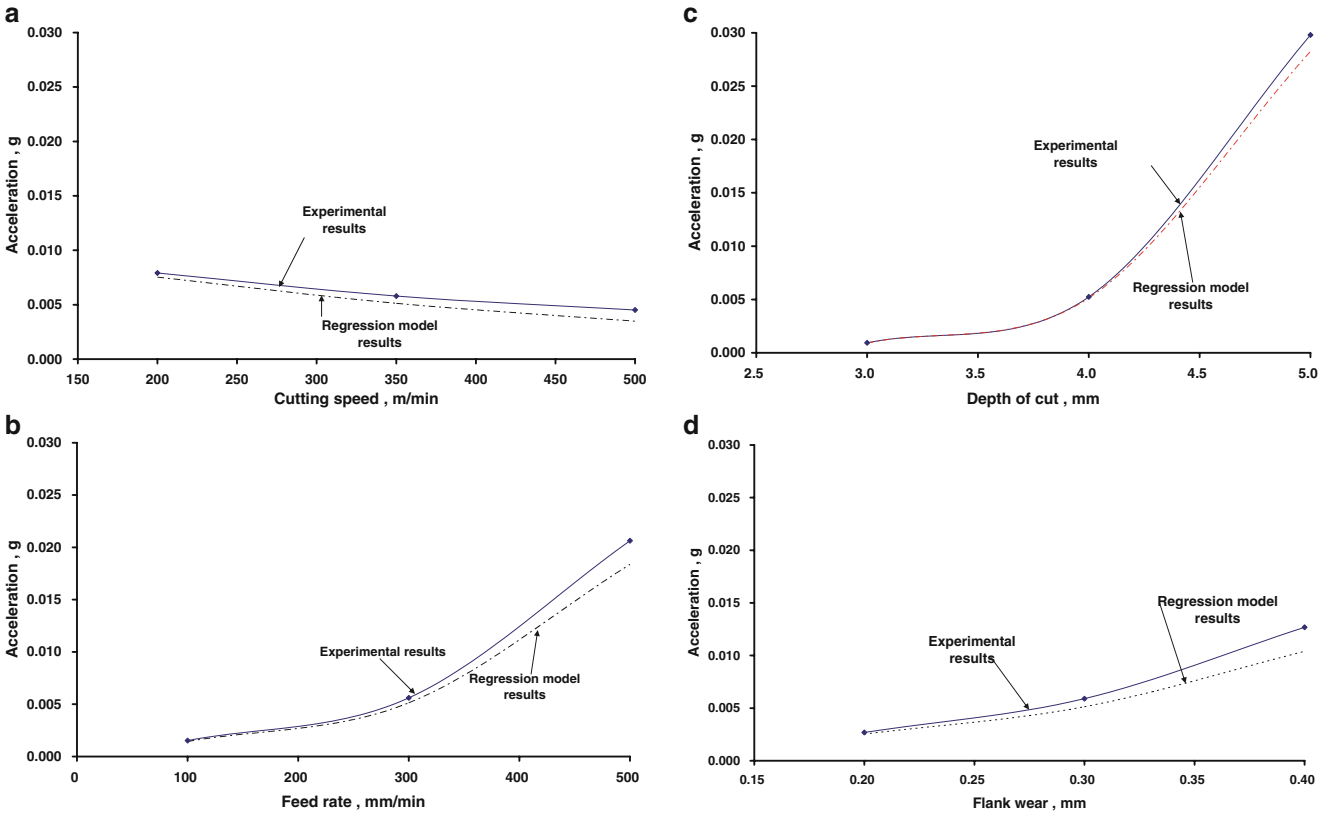

Fig. 11 **a** Variation of vibration levels, *g* vs. cutting speed (channel 1 feed rate=300 mm/min, depth of cut=4 mm and flank wear=0.3 mm). **b** Variation of vibration levels, *g* vs. feed rate (channel 1 cutting speed=350 mm/min, depth of cut=4 mm and flank wear=0.3 mm). **c** Variation of vibration levels, *g* vs. depth of cut (channel 1 cutting speed=350 m/min, feed rate=300 mm/min and flank wear=0.3 mm). **d** Variation of vibration levels, *g* vs. flank wear (channel 1 cutting speed=350 m/min, feed rate=300 mm/min and depth of cut=4 mm)

terms of acceleration, *g* is small up to 0.3 mm flank wear level due to small variation in cutting force. In case of strain as a response, the variation in strain level is also low up to 0.3 mm flank wear level due to small variation (Fig. 10a) in cutting force, but there is sudden rise in strain beyond 0.3 mm flank wear due to increase in cutting force.

4.2 Effect of feed rate, cutting speed on acceleration, *g* and strain gauge bridge

The relationships between machining parameter feed rate and acceleration, *g* for various flank wear levels are shown in Figs. 8b (channel 1) and 9b (channel 2). The amplitude of vibration *g*, increases with increase in feed rate which results in increased dynamic cutting force. The increase in dynamic cutting force is associated with reduction in the stiffness of the cutting tool. The variation in strain level is low (Fig. 10b) up to 0.2 mm flank wear level due to small variation in cutting force. Similarly the effects of cutting speed for various flank wear levels are shown in Figs. 8c and 9c. Increase in cutting speed reduces the cutting force, and hence it will reduce the vibration and strain levels. The variation in strain level is low up to 0.2 mm flank wear level due to very small variation (Fig. 10c) in cutting force.

In statistical software Data*fit* (ANOVA) the 99% confidence intervals (α value) are chosen at various levels and best model values are shown in Appendix 2 (Tables 9, 10 and 11). From the ANOVA, all the values of $P \leq 0.01$ indicate that the effect of the parameter is significant. The detailed ANOVA has been made for each level of flank wear with respect to machining input parameters as shown in Appendix 2 (Table 9 Regression model I for channel 1). From the results of ANOVA (Appendix 2, Tables 9, 10 and 11), it is observed that F Ratios were large enough and indicate that the developed models are appropriate [14].

Out of five levels of flank wear, three levels (0.2, 0. 3 and 0.4 mm) were selected for the analysis of variance (ANOVA) to develop the regression models (Eqs. 2–4) to show the relationship between output response and machining input parameters. A model has four independent parameters for three dependent responses. Three models were tested for each channel output and the one which gave the highest coefficient of correlation was selected. The selected models for channel 1, channel 2 and channel 3 are

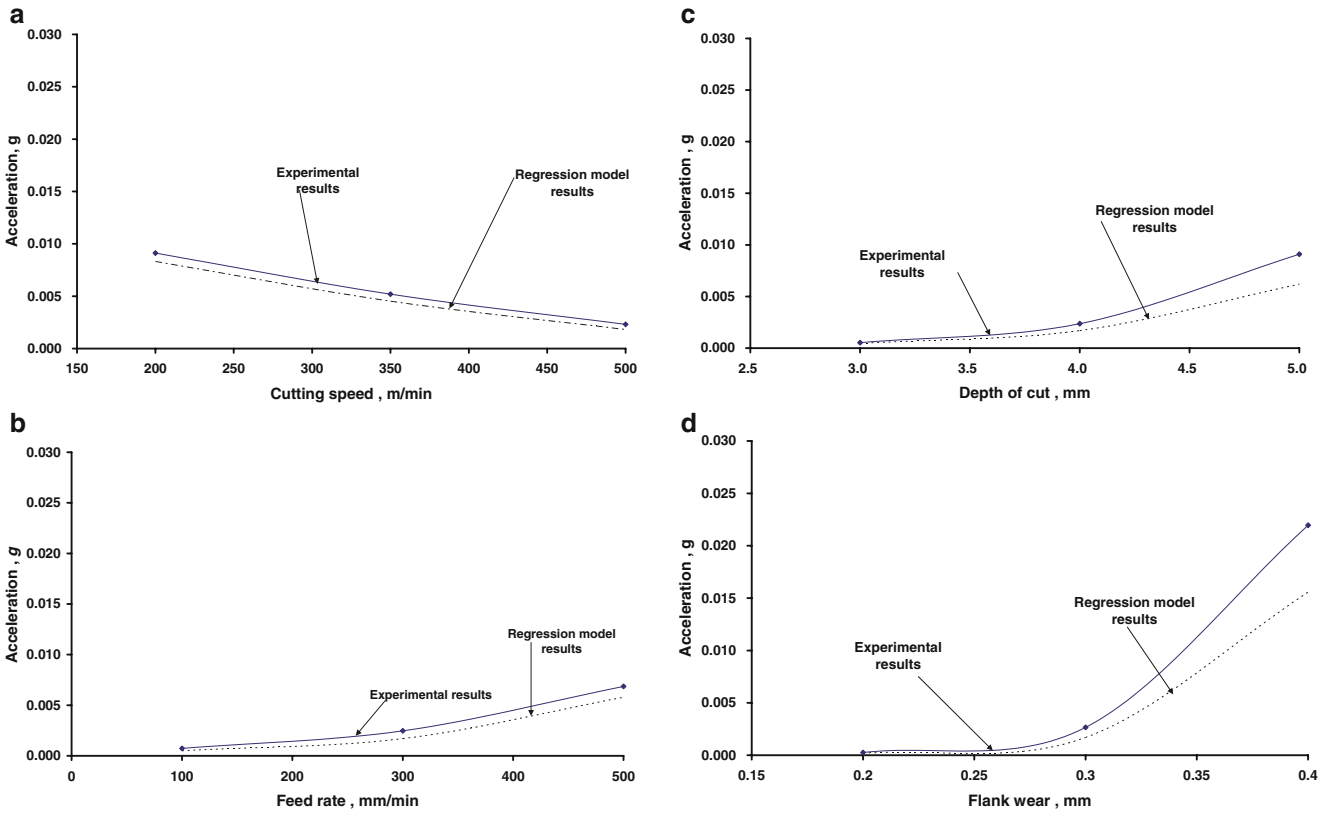

Fig. 12 **a** Variation of vibration levels, g vs. cutting speed (channel 2 feed rate=300 mm/min, depth of cut=4 mm and flank wear=0.3 mm). **b** Variation of vibration levels, *g* vs. feed rate (channel 2 cutting speed=350 mm/min , depth of cut=4 mm and flank wear=0.3 mm). **c** Variation of vibration levels, g vs. depth of cut (channel 2 cutting speed=350 m/min, feed rate=300 mm/min and flank wear=0.3 mm). **d** Variation of vibration levels, *g* vs. flank wear (channel 2 cutting speed=350 m/min, feed rate=300 mm/min and depth of cut=4 mm)

given by the Eqs. (2–4), respectively. These models gave higher value of F-ratio as compared to the tabulated F-ratio value which demonstrates that the selected models are appropriate. According to ANOVA response (F ratio, P and R^2 values) the best regression model has been chosen. To perform the parametric study using these regression models, the relationships have been drawn between the machining conditions and responses (acceleration, *g vs.* Cutting speed (Figs. 11a, 12a, 13a), acceleration, *g vs.* Feed rate (Figs. 11b, 12b and 13b) and so on).

$$\beta 1 = \exp\left(a_1 x_1 + b_1 x_2 + c_1 x_3 + d_1 x_4 + e_1\right) \quad (2)$$

$$\beta 2 = \exp\left(a_2 x_1 + b_2 x_2 + c_2 x_3 + d_2 x_4 + e_2\right) \quad (3)$$

$$\delta = \exp\left(a_3 x_1 + b_3 x_2 + c_3 x_3 + d_3 x_4 + e_3\right) \quad (4)$$

where, x_1= cutting speed, x_2= feed rate, x_3= depth of cut, x_4= flank wear, β_1= acceleration, *g* in cutting direction, β_2= acceleration, *g* in feed direction,δ = micro strain.

Following values of the various coefficients of Eqs. (2–4) have been obtained.

$a_1 = -2.565\ e-3,\ a_2 = -1.939\ e-3,$
$a_3 = -7.054\ e-3,\ b_1 = 6.739\ e-3,$
$b_2 = 6.137\ e-3,\ b_3 = 9.878\ e-3,\ c_1 = 1.706,$
$c_2 = 1.296,\ c_3 = 2.006,\ d_1 = 7.066,\ d_2 = 22.169,$
$d_3 = 6.538,\ e_1 = -15.233,\ e_2 = -20.734,$
$e_3 = -13.444$

The error between the regression model values and experimental values are calculated as

$$\varepsilon = \left|\frac{A_m - A_i}{A_m}\right| \times 100 \quad (5)$$

where,

ε error rate between experimental data and regression model data,
A_i the experimentally measured acceleration, *g* or micro strain,
A_m the predicted acceleration, *g* or micro strain from regression equations.

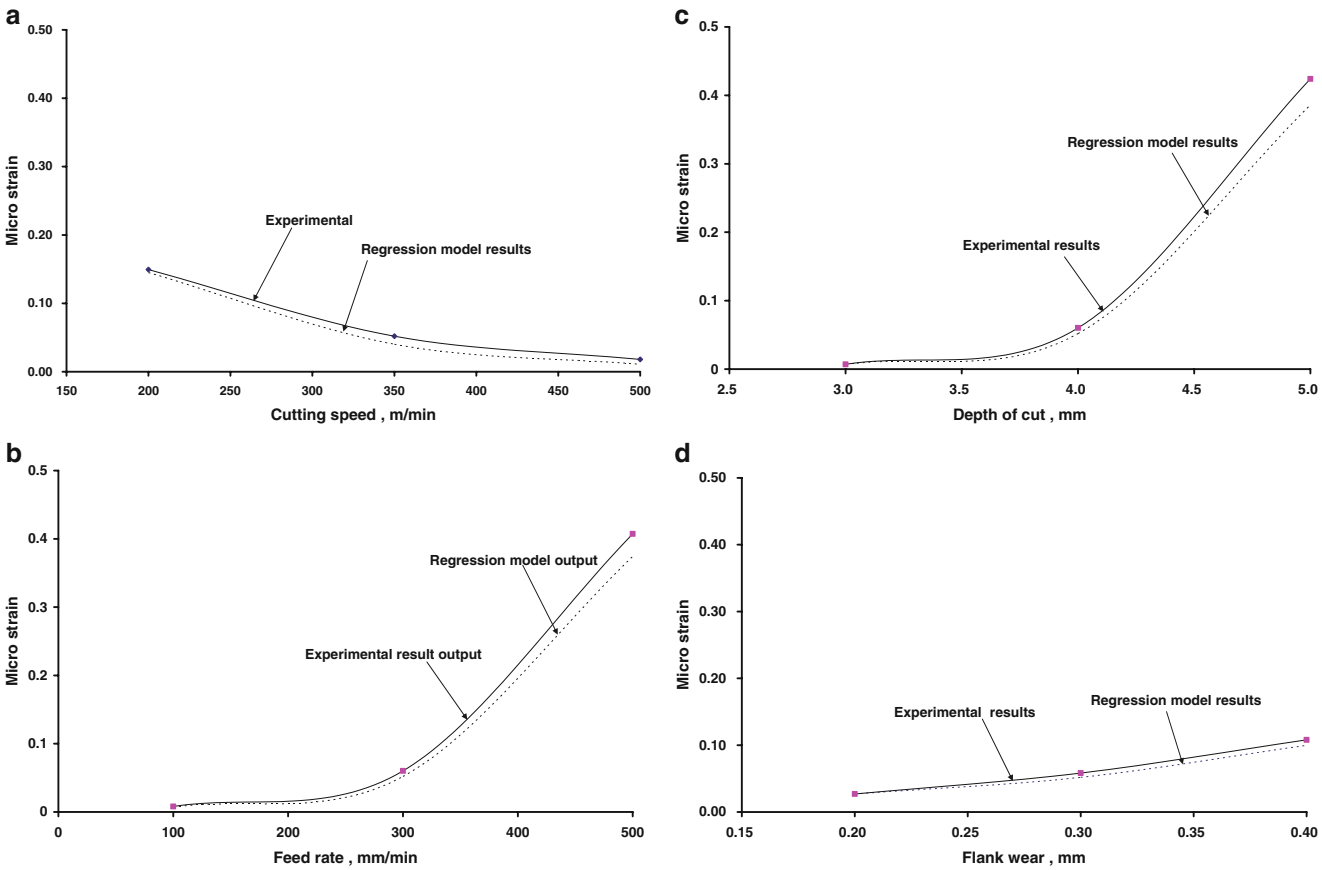

Fig. 13 **a** Variation of micro strain vs. cutting speed (channel 3 feed rate=300 mm/min , depth of cut=4 mm and flank wear=0.3 mm). **b** Variation of micro strain vs. feed rate(channel 3 cutting speed= 300 mm/min , depth of cut=4 mm and flank wear=0.3 mm). **c** Variation of micro strain vs. depth of cut (channel 3 cutting speed=350 m/min, feed rate=300 mm/min and flank wear=0.3 mm). **d** Variation of micro strain vs. flank wear(channel 3 cutting speed=350 m/min, feed rate= 300 mm/min and depth of cut=4 mm)

Table 3 Neural network architecture parameters

Trial No	Neural network architecture	No of epochs	Transfer function	Comments
1	100-100-100-100-5	20000	*logsig, logsig, logsig, logsig, tansig, logsig*	Not converged, it attained maximum epochs
2	110-110-110-110-5	20000	*logsig, logsig, logsig, logsig, tansig, logsig*	Not converged, it attained maximum epochs
3	120-120-120-120-5	7390	*logsig, logsig, logsig, logsig, tansig, logsig*	*Converged*
4	125-125-125-120-5	5386	*logsig, logsig, logsig, logsig, tansig, logsig*	*Converged*
5	125-125-125-125-5	20000	*logsig, logsig, logsig, logsig, tansig, logsig*	Not converged, it attained maximum epochs
6	130-130-130-120-5	4049	*logsig, logsig, logsig, logsig, tansig, logsig*	*Converged*
7	130-130-130-125-5	5029	*logsig, logsig, logsig, logsig, tansig, logsig*	*Converged*
8	130-130-130-130-5	9251	*logsig, logsig, logsig, logsig, tansig, logsig*	Training stopped due to non convergence
9	140-140-130-120-5	6351	*logsig, logsig, logsig, logsig, tansig, logsig*	Training stopped due to non convergence
10	140-140-130-125-5	3351	*logsig, logsig, logsig, logsig, tansig, logsig*	Training stopped due to non convergence
11	140-140-140-120-5	4051	*logsig, logsig, logsig, logsig, tansig, logsig*	Training stopped due to non convergence
12	150-140-130-120-5	6851	*logsig, logsig, logsig, logsig, tansig, logsig*	Training stopped due to non convergence
13	150-150-150-120-5	4901	*logsig, logsig, logsig, logsig, tansig, logsig*	Training stopped due to non convergence
14	150-150-150-150-5	20000	*logsig, logsig, logsig, logsig, tansig, logsig*	Not converged, it attained maximum epochs
15*	130-120-120-120-5	1863	*logsig, logsig, logsig, logsig, tansig, logsig*	***Converged***
16	120-120-120-120-5	4113	*logsig, logsig, logsig, logsig, tansig, logsig*	*Converged*
17	140-130-130-120-5	1851	*logsig, logsig, logsig, logsig, tansig, logsig*	Training stopped due to non convergence
18	130-120-120-100-5	2052	*logsig, logsig, logsig, logsig, tansig, logsig*	*Converged*
19	130-130-120-120-5	3311	*logsig, logsig, logsig, logsig, tansig, logsig*	*Converged*

*Trial No 15, the architecture of 130-120-120-120-5 gives best convergence, lower computation time and response of training and is good enough to classify the flank wear at various levels.

The error rate of channel 1 (β_1) of this model is calculated by using Eq. (5). The calculated values are 4.82% for the cutting speed 200 m/min, 11.41% for the cutting speed 350 m/min and 22.6% for the cutting speed 500 m/min. The deviations (or percentage of errors) increased with increase in cutting speed as shown in Figs. 11a, 12a, and 13a. This increasing error may be due to measurements errors in the sensors at high cutting frequencies. The error rate or deviations rate increase with increase in feed rate as shown in Figs. 11b, 12b and 13b, which is due to variation in dynamic cutting conditions and increase in cutting force. If cutting force increases the distortion of amplitude also increases in both accelerometer and strain gauge bridge. Similarly error values increase with increase in depth of cut (shown in Figs. 11c, 12c and 13c) as well as increase in flank wear (Figs. 11d, 12d and 13d). This is due to increase in cutting force as discussed above.

Table 4 Typical training output vectors (target vectors)

	Flank wear levels				
	0.5 mm	***0.4 mm***	***0.3 mm***	***0.2 mm***	***0.0 mm***
Output vectors	1	0	0	0	0
	0	1	0	0	0
	0	0	1	0	0
	0	0	0	1	0
	0	0	0	0	1

5 Neural networks

Cutting tool wear and breakage have a direct influence on dynamic characteristics of any manufacturing process. Metal cutting processes are generally non-linear, time dependent, and vary with material properties and machining conditions. Neural networks are known to be a mathematical tool to handle such a dynamic and non linear phenomenon. Most of the researchers [2, 3, 5, 8] have used feed forward back propagation, self organizing maps (SOM), probabilistic neural networks (PNN) using either time domain or frequency domain signals. In past two decades [18, 19] wavelet transform technique has also been used in the area of cutting tool condition monitoring system. A real condition monitoring system is expected to replace the knowledge and experience of a skilled machine operator. This can be achieved through proper learning and training of artificial neural network (ANN) [20]. Neural

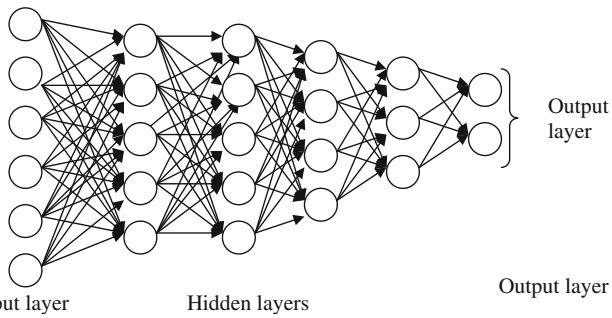

Fig. 14 Feed forward neural network with four hidden layer

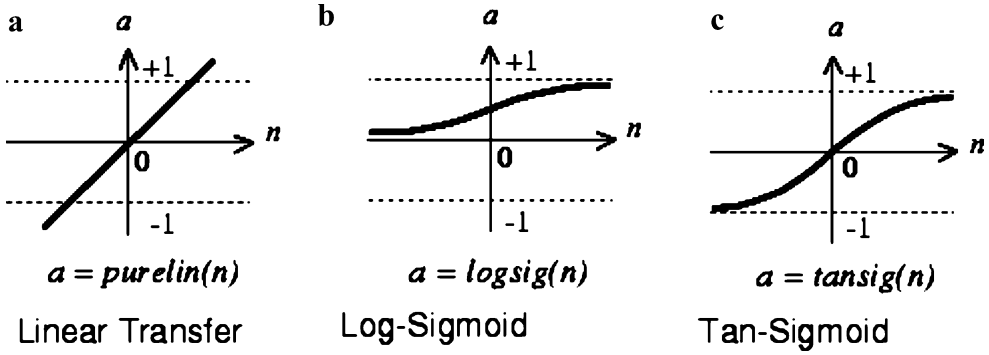

Fig. 15 Transfer functions. **a** Purelin transfer function. **b** Logsig transfer function. **c** Tansig transfer function

network-based condition monitoring systems [21] employ feed forward multi-layer perceptrons (MLP).

In this study, an attempt has been made to estimate the flank wear using MLP architecture. In multi layer perceptron [2], the neural network architecture, number of layers, nodes, transfer function and training pattern are conveniently chosen as shown in Table 3. The feed forward back propagation algorithm is chosen for training and testing the experimental data. We have conducted 27 experiments with different combinations of machining conditions. On taking flank wear levels of 0, 0.2, 0.3, 0.4 & 0.5 mm as a parameter, the total number of experiments becomes 135 (=27×5). Out of these, 110 experiments with different machining conditions have been selected for training and remaining 25 experiments are reserved for testing. Additionally, training algorithms, number of nodes, transfer functions and number of layers are varied to study the behaviour of networks and to arrive at an optimum configuration.

The output signals of three sensors were used as input vectors to the neural networks. For single flank wear, the number of input terms in an input vector is 3 i.e., output responses of two accelerometers in terms of vibration amplitude, *g* in cutting, and feed directions, and third one is strain gauge bridge output.

The target vectors of neural networks are fixed as shown in Table 4. In Table 4, first column (1 0 0 0 0) indicates the level of flank wear as 0.5 mm. Similarly second, third, fourth, and fifth columns indicate the levels of flank wear as 0.4, 0.3, 0.2 and 0 mm, respectively.

In this work, six layers feed forward back propagation (Fig. 14) neural networks with one input, four hidden layers and one-output layer were used. The training is carried out for five levels of flank wear (0, 0.2, 0.3, 0.4 & 0.5 mm). Different combinations of architecture were tried out for five different levels of flank wear. Many transfer functions are available in Matlab toolbox. Three of them (*purelin, logsig, tansig)* are commonly used as transfer functions. The transfer function *purelin* is called linear transfer function and is shown in Fig. 15a. Neurons of *purelin* transfer function are used as linear approximators. A Sigmoid function is a mathematical function (Eq. 6) that produces a sigmoid curve ("S" shape). Often, sigmoid function refers to the special case of the logistic function and is defined by

$$f(x) = \frac{1}{1 + e^{-x}} \tag{6}$$

The sigmoid (*logsig* and *tansig)* transfer function (shown in Fig. 15b,c) takes the input, which may have any value between plus and minus infinity, and squashes the output into the range 0 to 1 *(logsig)* or −1 to 1 *(tansig)*. Investigations were carried out with a variety of transfer functions like *tansig, logsig, purelin* etc for the activation function used to represent the neurons [22]. Similarly, back-propagation training algorithms like *traingd, traingda, traingdx, trainlm,trainrp* were tried. Best results were obtained with *logsig* and *tansig* activation function.

Table 5 Typical output for test data for Ex No 25 and 26

	Ex No 25					Ex No 26				
	Flank wear levels					Flank wear levels				
Output vectors	0.5 mm	0.4mm	0.3 mm	0.2 mm	0.0 mm	0.5 mm	0.4 mm	0.3 mm	0.2 mm	0.0 mm
	1.000	0.000	0.000	0.002	−0.011	***1.000***	0.001	0.003	0.015	−0.037
	−0.003	***0.999***	0.000	−0.005	0.003	0.000	***0.988***	−0.002	0.076	0.058
	−0.001	−0.001	***0.991***	−0.004	0.011	0.001	−0.002	***0.992***	−0.004	0.000
	−0.001	0.000	−0.003	***0.991***	0.013	0.002	−0.002	0.000	***0.929***	0.024
	−0.001	−0.001	0.002	−0.005	***0.954***	0.005	−0.011	−0.003	0.002	***0.951***

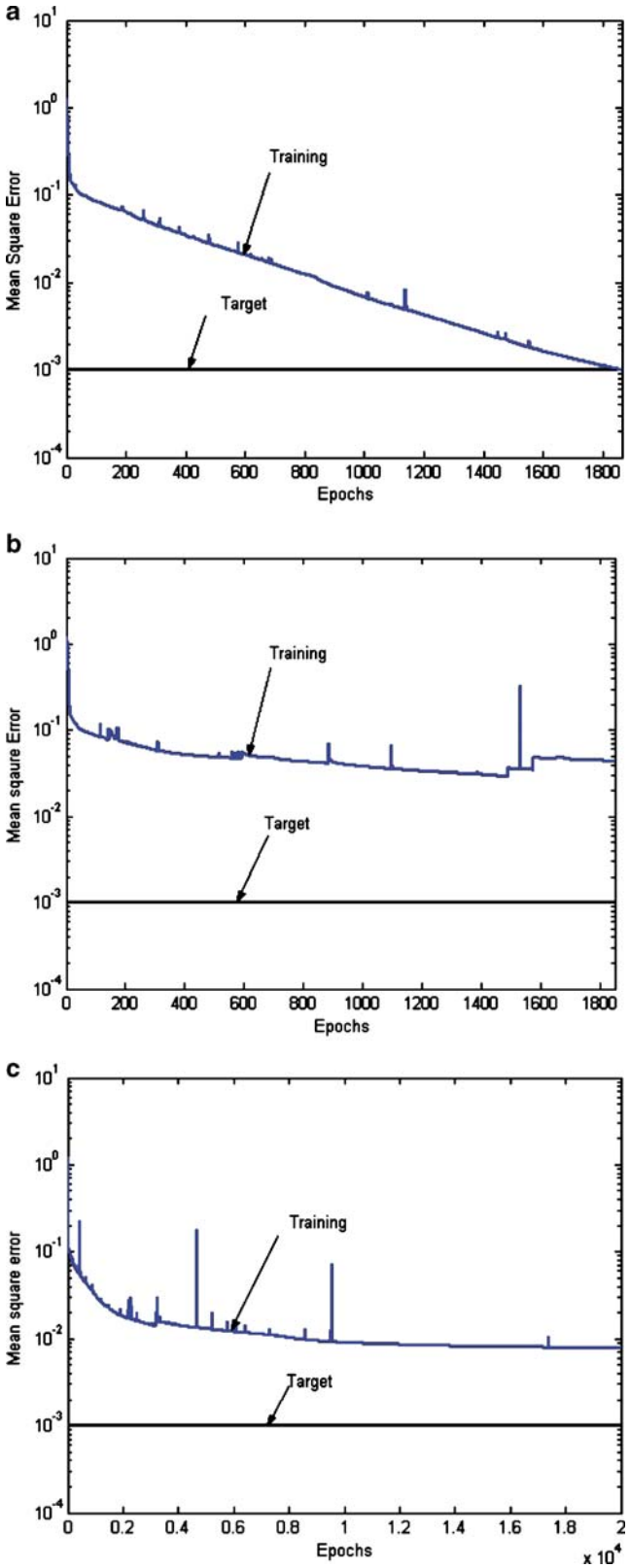

Fig. 16 **a** Convergence pattern of back propagation networks for Trial No 15. **b** Convergence pattern of back propagation networks for Trial No 17. **c** Convergence pattern of back propagation networks for Trial No 5

The *trainrp* is found to be most robust training algorithm in terms of accuracy and time taken. The performance of various neural network architectures have been analysed and some of them are described in Table 3. The behaviour of neural networks architecture depends upon various parameters like input patterns to networks, target vectors, number of layers, number of neurons, activation function, training function, number of epochs and so on. In this paper an attempt has been made to classify the flank wear levels by using ANN. In the Table 3, different combination of architecture were tried to find an optimal architecture. Out of these trials, Trial number 15 gives better convergence (Fig. 16a), less computation time and response of network is good enough to classify the flank wear levels. In trial No 17, the network is not allowed to run for 20000 epochs because the rate of divergence increases with increases in number of epochs (after 1,500 cycles) as shown in Fig. 16b. It never converged to achieve the target level of accuracy 1×10^{-3} within 20,000 epochs. On trial and error basis, the training of networks is allowed to run up to the maximum number of epochs like Trial No 5. But this trial did not converge to the target level as shown in Fig. 16c. Similarly, an attempt has been made to reduce the computational timings by selecting proper architecture of neural works (Trial No 15 of architecture 130-120-120-120-5). The same architecture was used for both training and testing the experimental data. The testing results are shown in Table 5 for the experiment numbers 25 and 26.

A neural network model has been developed and used to predict the condition of the cutting tool. On the basis of the condition of the cutting tool, this neural network model may be further employed to develop an adaptive feedback system to control the machining process.

6 Conclusions

The development of practical and reliable condition monitoring system for detecting flank wear in turning operation is essential for realization of intelligent and flexible manufacturing systems. In this study, the problem of detection of flank wear in turning operation has been studied using vibration and strain measurement methods. Based on the current study, the following conclusions can be drawn:

Artificial wear can be created in a controlled manner by using EDM process, which emulates the real flank wear.

Vibration and strain monitoring during turning operation can be useful for predicting flank wear. For this purpose, frequency domain analyses have been carried out and features were fed in to ANN as input data. The response of ANN is good enough to classify the flank wear at different levels.

The neural networks code was tested employing various training algorithms available in the Matlab toolbox and finally optimum architecture (Trial No 15) was selected. Among these algorithms, the *trainrp* was found to be most robust and easily applicable to classify the flank wear levels while using *logsig* and *tansig* as activation functions.

A multiple regression model has been developed and validated with experimental results.

Acknowledgement The authors acknowledge the contribution of Dr.V.Raghuram, Principal Research Engineer, for valuable suggestion while conducting experiments and Mr.T.V.K.Gupta, Research Engineer, who is giving constant support to carry out experiments as well as analysis part.

Appendix 1

Table 6 Input parameters - dynamic response of accelerometer (channel 1) in cutting direction

Experimental conditions				Amplitude of acceleration, g for different level of flank wears				
Ex No	CS	FR	DOC	0.5 mm FW	0.4 mm FW	0.3 mm FW	0.2 mm FW	0.0 mm FW
1	500	500	5	0.2330	0.1580	0.0298	0.0091	0.0107
2	500	500	4	0.0528	0.0079	0.0131	0.0043	0.0026
3	500	500	3	0.0456	0.0196	0.0026	0.0009	0.0020
4	500	300	5	0.0759	0.0298	0.0132	0.0113	0.0070
5	500	300	4	0.0389	0.0079	0.0050	0.0058	0.0012
6	500	300	3	0.0348	0.0035	0.0047	0.0023	0.0014
7	500	100	5	0.0492	0.0033	0.0019	0.0028	0.0061
8	500	100	4	0.0310	0.0029	0.0019	0.0020	0.0031
9	500	100	3	0.0238	0.0013	0.0003	0.0006	0.0005
10	350	500	5	0.2750	0.2330	0.1050	0.0199	0.0111
11	350	500	4	0.2000	0.0200	0.0219	0.0053	0.0036
12	350	500	3	0.0316	0.0111	0.0038	0.0030	0.0034
13	350	300	5	0.2530	0.0456	0.0247	0.0128	0.0083
14	350	300	4	0.1540	0.0187	0.0090	0.0085	0.0061
15	350	300	3	0.0275	0.0052	0.0074	0.0043	0.0016
16	350	100	5	0.1890	0.0348	0.0105	0.0066	0.0064
17	350	100	4	0.0691	0.0115	0.0097	0.0009	0.0039
18	350	100	3	0.0107	0.0008	0.0026	0.0011	0.0009
19	200	500	5	0.2650	0.2650	0.2320	0.0345	0.0153
20	200	500	4	0.2320	0.0585	0.0241	0.0090	0.0095
21	200	500	3	0.1760	0.0065	0.0092	0.0087	0.0052
22	200	300	5	0.2410	0.0621	0.0261	0.0442	0.0132
23	200	300	4	0.1630	0.0389	0.0110	0.0098	0.0091
24	200	300	3	0.1580	0.0076	0.0058	0.0045	0.0019
25	200	100	5	0.1060	0.0613	0.0145	0.0129	0.0112
26	200	100	4	0.0613	0.0186	0.0098	0.0092	0.0053
27	200	100	3	0.0186	0.0042	0.0077	0.0051	0.0037

CS = cutting speed in m/min, FR= feed rate in mm/min, DOC = depth of cut in mm and FW = flank wear in mm

Table 7 Input parameters - dynamic response of accelerometer (channel 2) in feed direction

Experimental conditions				Amplitude of acceleration, g for different level of flank wears				
Ex No	CS	FR	DOC	0.5 mm FW	0.4 mm FW	0.3 mm FW	0.2 mm FW	0.0 mm FW
1	500	500	5	0.2670	0.2450	0.0103	0.0089	0.0068
2	500	500	4	0.2370	0.0883	0.0065	0.0058	0.0037
3	500	500	3	0.1570	0.0277	0.0035	0.0025	0.0017
4	500	300	5	0.0939	0.0638	0.0071	0.0061	0.0040
5	500	300	4	0.0448	0.0191	0.0049	0.0051	0.0031
6	500	300	3	0.0239	0.0087	0.0024	0.0017	0.0025
7	500	100	5	0.0457	0.0229	0.0040	0.0033	0.0033
8	500	100	4	0.0408	0.0059	0.0028	0.0028	0.0024
9	500	100	3	0.0191	0.0065	0.0015	0.0007	0.0019
10	350	500	5	0.2480	0.2370	0.0210	0.0136	0.0077
11	350	500	4	0.2450	0.0389	0.0086	0.0061	0.0054
12	350	500	3	0.1640	0.0110	0.0054	0.0033	0.0044
13	350	300	5	0.2490	0.0627	0.0100	0.0070	0.0054
14	350	300	4	0.1900	0.0122	0.0066	0.0058	0.0034
15	350	300	3	0.1430	0.0057	0.0033	0.0021	0.0027
16	350	100	5	0.0929	0.0264	0.0050	0.0053	0.0037
17	350	100	4	0.0264	0.0055	0.0036	0.0029	0.0028
18	350	100	3	0.0249	0.0045	0.0031	0.0007	0.0025
19	200	500	5	0.2710	0.1210	0.0226	0.0194	0.0083
20	200	500	4	0.2640	0.0239	0.0123	0.0094	0.0067
21	200	500	3	0.1690	0.0017	0.0085	0.0037	0.0051
22	200	300	5	0.2330	0.0408	0.0159	0.0125	0.0061
23	200	300	4	0.1470	0.0063	0.0120	0.0084	0.0041
24	200	300	3	0.1310	0.0039	0.0062	0.0045	0.0034
25	200	100	5	0.1920	0.0167	0.0127	0.0064	0.0049
26	200	100	4	0.1330	0.0249	0.0089	0.0033	0.0032
27	200	100	3	0.0601	0.0044	0.0081	0.0010	0.0028

Table 8 Input parameters - dynamic response of strain gauge (channel 3)

Experimental conditions				Micro strain for different level of flank wears				
Ex No	CS	FR	DOC	0.5 mm FW	0.4 mm FW	0.3 mm FW	0.2 mm FW	0.0 mm FW
1	500	500	5	7.4488	4.2373	0.0141	0.02108	0.001350
2	500	500	4	0.0274	0.1118	0.0013	0.00566	0.000378
3	500	500	3	0.0100	0.0017	0.0006	0.00229	0.000234
4	500	300	5	0.8566	0.0210	0.0025	0.00736	0.001245
5	500	300	4	0.0224	0.0031	0.0011	0.00174	0.000166
6	500	300	3	0.0017	0.0011	0.0002	0.00053	0.000020
7	500	100	5	0.0500	0.3906	0.0007	0.00004	0.000749
8	500	100	4	0.0141	0.0079	0.0003	0.00056	0.000148
9	500	100	3	0.0015	0.0010	0.0003	0.00009	0.000138
10	350	500	5	13.972	5.7864	0.3940	0.02123	0.269500
11	350	500	4	0.5940	0.0141	0.0727	0.01852	0.001401
12	350	500	3	0.1176	0.0045	0.0061	0.01562	0.000265
13	350	300	5	1.0856	1.8221	0.1274	0.01791	0.013886

Table 8 (continued)

Experimental conditions				Micro strain for different level of flank wears				
Ex No	CS	FR	DOC	0.5 mm FW	0.4 mm FW	0.3 mm FW	0.2 mm FW	0.0 mm FW
14	350	300	4	0.3371	0.0104	0.0241	0.00196	0.000343
15	350	300	3	0.0727	0.0017	0.0159	0.00108	0.000159
16	350	100	5	0.0637	0.0797	0.0014	0.00014	0.000803
17	350	100	4	0.0485	0.0100	0.0012	0.00064	0.000286
18	350	100	3	0.0270	0.0012	0.0007	0.00096	0.000002
19	200	500	5	14.168	13.9720	12.8480	0.65594	0.367030
20	200	500	4	4.2373	0.3184	5.6611	0.01325	0.015560
21	200	500	3	0.3217	0.0727	0.0168	0.00064	0.006222
22	200	300	5	2.4882	2.4882	0.4354	0.02416	0.019056
23	200	300	4	0.4334	0.0141	0.0322	0.00437	0.012440
24	200	300	3	0.1361	0.0036	0.0199	0.00038	0.004686
25	200	100	5	0.1450	0.0985	0.0110	0.00303	0.000729
26	200	100	4	0.0943	0.0284	0.0011	0.00080	0.001429
27	200	100	3	0.0286	0.0017	0.0009	0.00049	0.000128

Appendix 2

Table 9 ANOVA for effect of machining parameters with respect to dynamic response of accelerometer in cutting direction (channel 1)

Source	DF	SS	MS	F	P
Regression	4	0.17390	4.34762E-02	166.0451346	0
Residual Error	76	1.9899E-02	2.61833E-04		
Total	80	0.1938043			
Predictor	**Coef**	**SE Coef**	**T**	**P**	
Constant	−15.23397	0.987513	−15.4266	0.0	
Cutting speed	−2.56E-03	3.218870E-04	−7.969620	0.0	
Feed rate	6.37E-03	5.8018617E-04	10.996413	0.0	
Depth of cut	1.706460	0.1836045	9.2942163	0.0	
Flank wear	7.063323	0.63513239	11.121026	0.0	
Source	DF		Coefficient of multiple determination (R^2) = 0.8973223476		
Cutting speed	1				
Feed rate	1				
Depth of cut	1				
Flank wear	1				

Table 10 ANOVA for effect of machining parameters with respect to dynamic response of accelerometer in feed direction (channel 2)

Source	DF	SS	MS	F	P
Regression	4	0.123439262	3.08598E-02	352.0307407	0
Residual Error	76	6.662332913E-03	8.76622E-05		
Total	80	0.1301015955			
Predictor	**Coef**	**SE Coef**	**T**	**P**	
Constant	−20.7342	0.9838920	−21.07369	0.0	
Cutting speed	1.939E-03	2.13193979E-04	9.099049645	0.0	
Feed rate	6.137E-03	3.86197506E-04	15.89108878	0.0	
Depth of cut	1.296833428	8.32526262E-02	15.57708731	0.0	
Flank wear	22.162948554	2.182573027	10.15450492	0.0	
Source	**DF**		Coefficient of multiple determination (R^2) = 0.94879		
Cutting speed	1				
Feed rate	1				
Depth of cut	1				
Flank wear	1				

Table 11 ANOVA for effect of machining parameters with respect to dynamic response of strain gauge bridge (channel 3)

Source	DF	SS	MS	F	P
Regression	4	343.3472	85.83681	81.3959	0
Residual Error	76	80.14645	1.054558		
Total	80	423.4936			
Predictor	**Coef**	**SE Coef**	**T**	**P**	
Constant	−13.444032	2.185416	−6.151702	0.0	
Cutting speed	−7.05427E-03	9.45E-04	−7.457052	0.0	
Feed rate	9.878094E-03	1.88E-03	5.2537984	0.0	
Depth of cut	2.00664334	0.388271	5.1681438	0.0	
Flank wear	6.53810364	0.934249	6.9982416	0.0	
Source	**DF**		Coefficient of multiple determination (R^2) = 0.81075		
Cutting speed	1				
Feed rate	1				
Depth of cut	1				
Flank wear	1				

References

1. Daniel Kriby E, Zhang Zhe, Chen JC (2004) Development of an accelerometer-based surface roughness prediction system in turning operations using multiple regression techniques. J ind technol 20(4):1–8
2. Dimla DE, Lister PM, Leighton NJ (2000) Neural networks solutions to the tool condition monitoring problem in metal cutting - A critical review of methods. Int j mach tools manuf 40:1219–1241
3. Dimla DE (2000) Sensors signals for tool-wear monitoring in metal cutting operations - A Review of methods. Int j mach tools manuf 40:1073–1098

4. Xiaoli Li (2002) A brief review: acoustic emission method for tool wear monitoring during turning. Int j mach tools manuf 42:157–165
5. Jemielniak K (1999) Commercial Tool condition monitoring systems. Int j adv manuf technol 15(4):711–721
6. Xiaoli Li (2002) A brief review: acoustic emission method for tool wear monitoring during turning. Int j mach tools manuf 42:157–165
7. Ghasempoor A, Jeswiet J, Moore TN (1999) Real time implementation of on line tool condition monitoring in turning. Int j mach tools manuf 39:1883–1902
8. Byrne G, Dornfeld D, Insaki I, Ketteler G, König W, Teti R (1995) Tool condition monitoring (TCM) – The status of research and industrial application. Annals of CIRP 44(2):541–567
9. Sick B (2002) On line and indirect tool wear monitoring in turning with artificial neural networks: A review of more than a decade of research. Mech syst signal process 16(4):487–546
10. Scheffer C, Kratz H, Heyns PS, Klocke F (2003) Develpoment of tool wear monitoring system for hard turning. Int j mach tools manuf 43:973–985
11. Kurada S, Bradley C (1997) A review of machine vision sensors for tool condition monitoring. Comput ind 34:55–72
12. Sunilkumar Kakade, Vijayaraghavan L, Krishnamurthy R (1995) Monitoring of tool status using intelligent acoustic emission sensing and decision based neural network. IEEE:25–29
13. Sen GC, Bhattacharyya A (1969) Principles of Metal Cutting, New Central Book Agency, New Delhi
14. Cochran WG, Cox GM (1962) Experimental Designs. Wiley, New York
15. Williams JE, Raja KK (2002) The effects of corner radius and edge radius on tool flank wear. J manuf process (SME) 4(2):89–95
16. Thomas M, Beauchamp Y (2003) Statistical investigation of modal parameters of cutting tools in dry turning. Int j mach tools manuf 43(11):1093–1106
17. Niu YM, Wong YS, Hong GS (1998) An intelligent sensor system approach for reliable tool flank wear recognition. Int j adv manuf Technol 14:77–84
18. Lee BY, Tarng YS (2004) Application of the discrete wavelet transform to the monitoring of tool failure in end milling using the spindle motor. Int j adv manuf technol 15(4):238–243
19. Scheffer C, Heyns PS (2001) Wear monitoring in turning operations using vibration and strain measurements. Mech syst signal process 15(6):1185–1202
20. Rangwala S, Dornfeld D (August 1990) Sensor Integration using neural networks for intelligent tool condition monitoring. J eng ind 112:219–228
21. Ozel T, Nadgir A (2002) Prediction of flank wear by using neural networks modeling when cutting hardened H-13 steel with chamfered and honed CBN tools. Int j mach tools manuf 42:287–297
22. Zurada JM (1999) Introduction to Artificial Neural Systems, Jaico Publishing House, New Delhi